Accepted Manuscript

CdS particles modified TiO2 coatings formed by plasma electrolytic oxidation with enhanced photocatalytic activity

Stevan Stojadinović, Nenad Tadić, Nenad Radić, Boško Grbić, Rastko Vasilić

PII: S0257-8972(18)30331-1
DOI: doi:10.1016/j.surfcoat.2018.03.080
Reference: SCT 23260

To appear in: *Surface & Coatings Technology*

Received date: 16 January 2018
Revised date: 26 February 2018
Accepted date: 26 March 2018

Please cite this article as: Stevan Stojadinović, Nenad Tadić, Nenad Radić, Boško Grbić, Rastko Vasilić , CdS particles modified TiO2 coatings formed by plasma electrolytic oxidation with enhanced photocatalytic activity. The address for the corresponding author was captured as affiliation for all authors. Please check if appropriate. Sct(2017), doi:10.1016/j.surfcoat.2018.03.080

CdS particles modified TiO_2 coatings formed by plasma electrolytic oxidation with enhanced photocatalytic activity

Stevan Stojadinović[a*], Nenad Tadić[a], Nenad Radić[b], Boško Grbić[b], Rastko Vasilić[a]

[a] *University of Belgrade, Faculty of Physics, Studentski trg 12-16, 11000 Belgrade, Serbia*

[b] *University of Belgrade, Institute of Chemistry, Technology and Metallurgy, Department of Catalysis and Chemical Engineering, Njegoševa 12, 11000 Belgrade, Serbia*

*Corresponding author. Tel: + 381-11-7158161; Fax: + 381-11-3282619

E-mail address: sstevan@ff.bg.ac.rs (Stevan Stojadinović)

Abstract

CdS particles modified anatase TiO_2 photocatalysts were formed on titanium substrate by plasma electrolytic oxidation for 2 min in supporting electrolyte (10 g/L $Na_3PO_4 \cdot 12H_2O$) with addition of CdS particles in concentrations up to 8 g/L. Content of CdS particles incorporated into TiO_2 coatings depends of CdS particles concentration in supporting electrolyte, while surface morphology, phase structure and absorption properties of formed coatings were not significantly influenced by the addition of CdS particles. In contrast to pure TiO_2 coatings, TiO_2/CdS coatings exhibit enhanced photocatalytic activity (PA) in the degradation of methyl orange, used as a model organic pollutant, under simulated solar irradiation. The highest PA was observed for TiO_2/CdS coating formed in supporting electrolyte with addition of 0.4 g/L of CdS particles. Photoluminescence measurements indicate that enhanced PA is related to the reduction of the recombination rate of photogenerated electron/hole pairs as a result of TiO_2 and CdS coupling.

Keywords: Plasma Electrolytic Oxidation; Photocatalysis; TiO_2; CdS.

1. Introduction

Environmental pollution is one of the major global challenges. Semiconductor photocatalysis is the most efficient method for decomposition of organic pollutants in aqueous media [1]. Among various semiconductor photocatalysts, TiO_2 has attracted much attention due to its outstanding properties such as low cost, strong oxidizing power, nontoxicity, photostability, and chemical inertness [2]. However, practical application of TiO_2 in photocatalytic reactions is obstructed by two essential drawbacks: wide energy gap (3–3.2 eV) that limits its application to ultraviolet region and fast recombination of electron–hole pairs, which are generated after photon absorption when TiO_2 is irradiated with energy equal to or higher than its band gap [3]. Several strategies have been adopted for improving the photocatalytic efficiency of TiO_2. They can be summarized as either changing the energy structure of TiO_2, i.e., extending its optical absorption range from ultraviolet to visible region or decreasing the electron/hole recombination rate [4].

An effective method for improving the photocatalytic efficiency of TiO_2 is its coupling with wide band gap semiconductors such as WO_3, V_2O_5, SnO_2, CdS, CdSe, etc. [5]. CdS has relatively low band gap energy (~2.3 eV) and its mixing with TiO_2 enhances the photocatalytic activity of TiO_2/CdS system not only because of promotion of visible light absorption, but it also features better separation of photogenerated electron–hole pairs [6-8].

Up to now, hydrothermal method [9], liquid ion-exchange technique [10], sol–gel method [11], solvothermal method [12], etc. have been used to prepare TiO_2/CdS photocatalysts. In this work, we have utilized high-voltage plasma electrolytic oxidation (PEO) process [13,14] of titanium in alkaline electrolyte containing CdS particles for the formation of TiO_2/CdS photocatalysts. Generally, PEO is considered a valuable pathway for the formation of mixed oxide coatings. High temperatures and pressures present inside of

micro-discharging channels cause melting of the substrate material which reacts with much cooler electrolyte, thus solidifying and crystallizing quickly upon being ejected from the micro-discharging channel. This process repeats randomly over the substrate surface, resulting in the formation of relatively uniform oxide coating [14]. In-situ incorporation of particles into the PEO coatings has been explored as a new strategy to provide coatings with a wide range of compositions and functionalities [15]. CdS particles have negative zeta potential in alkaline media [16] which promotes their movement towards the titanium anode. CdS particles have melting point around 1750 °C, hence locally high temperature induced at micro-discharging sites (~5000 °C) during PEO of titanium [17] should result in deposition of CdS particles on the surface of coatings.

2. Experimental details

Titanium samples of dimensions 2.5 cm × 1 cm × 0.025 cm were obtained from 99.95% purity titanium sheet. Samples were ultrasonically cleaned in acetone and distilled water, dried in a warm air stream and sealed with insulation resin leaving only surface of 1.5 cm × 1 cm available to the electrolyte. The experimental setup used for PEO is described in Ref. [18]. Water solution of 10 g/L sodium phosphate dodecahydrate ($Na_3PO_4 \cdot 12H_2O$) was used as a supporting electrolyte. High purity CdS powder (Sigma Aldrich) was added to supporting electrolyte in concentrations up to 8 g/L. Since CdS particles are insoluble in supporting electrolyte and only freshly prepared electrolyte was used, PEO processing is conducted under identical conditions in each run. Temperature of the electrolyte was maintained at (10 ± 1) °C during PEO. Titanium samples were anodized at constant current density of 150 mA/cm^2 for 2 min.

Surface morphology was studied by scanning electron microscope (SEM) JEOL 840A equipped with energy dispersive x-ray spectroscopy (EDS). The ratio of titanium and cadmium in formed coatings was determined using a Shimadzu XRF-1800 wavelength dispersive x-ray fluorescence spectrometer. Crystalline phases were identified by x-ray diffraction (XRD) in Bragg–Brentano geometry using a Rigaku Ultima IV diffractometer. The Raman spectra were excited using the 532 nm diode solid state laser (laser power of 10 mW) on a Thermo Scientific DXR Raman microscope equipped with research optical microscope and CCD detector. UV–Vis diffuse reflectance spectra (DRS) were recorded using a UV–Vis spectrophotometer (Shimadzu UV-3600) while photoluminescence (PL) spectra were recorded using a Horiba Jobin Yvon Fluorolog FL3-22 spectrofluorometer, with Xe lamp as the excitation light source at room temperature. The size of CdS particles was measured by a laser light scattering particle size analyzer (Mastersizer 2000; Malvern Instruments Ltd., Malvern, Worcestershire, UK).

For photocatalytic activity evaluation of TiO_2/CdS coatings, the photodegradation of aqueous methyl orange (MO) solution at room temperature under simulated solar irradiation was used as a model reaction. The experimental setup and procedures used for photocatalytic measurement are described in Ref. [19]. In short, photocatalysts of dimensions 15 mm × 10 mm (active surface) were immersed into 10 mL of 8 mg/L aqueous MO solution. Prior to illumination, the solution and the catalysts were magnetically stirred in the dark for 30 min to achieve adsorption–desorption equilibrium. The photocatalytic measurements were performed using a 300 W lamp that simulates solar radiation (Solimed BH Quarzlampen) which was placed 25 cm above the surface of the dye solution. The evolution of MO concentration was monitored by measuring the variation of the intensity of main absorption peak at 464 nm. UV–Vis absorption measurements as a function of the light exposure time were performed using spectrophotometer Thermo Electron Nicolet Evolution 500. Also, the MO solution was

tested for photolysis in the absence of the photocatalyst in order to examine its stability. The lack of change in the MO concentration after 12 h of irradiation revealed that MO was stable under applied conditions and that degradation was only due to the presence of photocatalyst.

3. Results and discussion

Size distribution of CdS particles added to supporting electrolyte is shown in Fig. 1. The largest number of particles have diameter around (0.27 ± 0.1) μm. The surface morphology of coatings formed in supporting electrolyte with addition of CdS particles is characterized by numerous micro-discharge channels of varying diameter, as well as regions resulting from the rapid cooling of molten material (Fig. 2). It can also be noted that surface morphology is not significantly influenced by the concentration of CdS particles in supporting electrolyte. Typical cross-sectional SEM image of formed coatings is showed in Fig. 3. Dense coating, tightly adhered to the titanium substrate, with corresponding thickness of about (3.6 ± 0.3) μm, is formed after 2 min of PEO processing.

XRD pattern of pure CdS powder and XRD patterns of coatings formed in supporting electrolyte with addition of various concentrations of CdS particles are shown in Fig. 4. The peaks observed in XRD patterns of CdS particles at 2θ values of 26.5, 43.8, and 51.9 degrees, unambiguously match (111), (220), and (311) crystalline planes of the face centered cubic structure of CdS (PDXL DB Card No. 9008839). Fig. 4 also shows that obtained coatings are well crystallized with clearly pronounced diffraction peaks corresponding to anatase phase of TiO_2 (PDXL DB Card No. 9008213), which is the photocatalytically active phase. The absence of visible peaks corresponding to CdS in XRD patterns is a consequence of low concentration of CdS particles which are uniformly dispersed all over the TiO_2 surface coatings. In order to investigate whether CdS particles are present in TiO_2 coatings, we

performed Raman spectroscopy measurements (Fig. 5). Raman spectrum of CdS powder (Fig. 3a) is characterized by a strong band at about 296 cm^{-1} assigned to the first-order longitudinal optical phonon (1LO) and a peak at about 592 cm^{-1} corresponding to the second-order (2LO) optical phonon [20]. The dominant modes in the Raman spectra of pure TiO_2 coating at about 144 cm^{-1} (Eg(1)), 197 cm^{-1} (Eg(2)), 395 cm^{-1} (B1g(1)), 514 cm^{-1} (A1g, B1g(2)), and 637 cm^{-1} (Eg(3)) can be assigned to the Raman active modes of the anatase crystal phase [21]. Bands originating from both TiO_2 coating and CdS particles can be identified in Raman spectra of coatings formed in supporting electrolyte with addition of CdS particles, thus confirming the presence of CdS particles in TiO_2 coatings. High resolution SEM image of coating formed in electrolyte with addition of 8 g/L CdS particles shows that areas with high agglomeration of CdS particles can be found on the coating surface (Fig. 6), suggesting inert incorporation of CdS particles in PEO coatings [15]. At the same time, regions with deficiency of CdS particles can also be observed.

Since the concentration of CdS particles in PEO coatings was either close to or below the detection limit of EDS system we used wavelength dispersive XRF measurements to obtain Ti/Cd ratio. XRF measurements show that the content of CdS in coatings increases with increasing concentration of CdS particles in supporting electrolyte (Table 1), i.e. the concentration of particles embedded in TiO_2 coating is controlled by the concentration of the particles in electrolyte.

The influence of concentration of CdS particles in supporting electrolyte on photocatalytic activity (PA) of PEO coatings is presented in Fig. 7. C_0 is the original concentration of MO and C is the concentration after time t. Obviously, PA varies with the concentration of CdS particles added to supporting electrolyte. TiO_2/CdS coatings formed in supporting electrolyte with addition of CdS particles up to 0.5 g/L show better PA than pure TiO_2 coating. It can be noted that the highest PA was observed for the coating formed in

supporting electrolyte with addition of 0.4 g/L of CdS particles. High concentration of CdS particles in supporting electrolyte significantly reduces photoactivity of prepared photocatalysts and even shows significantly lower values than those for pure TiO_2. This indicates that concentration of CdS particles has a considerable influence on PA of TiO_2/CdS coatings, i.e., there is an optimal concentration of CdS in TiO_2 coatings that can be related to the amount of CdS particles added to supporting electrolyte.

Given that the influence of CdS particles incorporated into TiO_2 coatings on the morphology and phase structure is negligible, the main contribution of CdS particles to the PA is either in extending the optical absorption range of TiO_2/CdS coatings or in preventing fast recombination process of photogenerated electron/hole pairs. Fig. 8 shows UV–Vis DRS spectra of pure CdS powder and prepared coatings formed in supporting electrolyte with various additions of CdS particles. Obviously, TiO_2/CdS coatings do not show absorption band edge shift towards the visible light region. All TiO_2/CdS coatings show the band edge at about 385 nm, while the band edge of CdS powder is at about 570 nm. The band gap energy of TiO_2/CdS coatings can be calculated by using the Kubelka–Munk:

$$F(R)=\frac{(1-R)^2}{2R}=\frac{\alpha}{S}, \tag{1}$$

where $R=10^{-A}$ is the reflectance of semiconductor and A is the absorbance, while α and S denote the absorption coefficient and the scattering coefficient, respectively. The energy dependence of α for semiconductors in the region near the absorption edge is given by the equation:

$$\alpha \propto \frac{(h\nu-E_g)^{\eta}}{h\nu}, \tag{2}$$

where ν is the frequency of the incident photon, h is the Planck constant, and E_g is the optical absorption edge energy. The exponent η is related to whether the band gap associated with the

transition of the electron is direct or indirect. Based on equations (1) and (2), plot $[F(R) \cdot h\nu]^{1/\eta}$ as a function of $h\nu$ (Tauc plot) is linear near the edge and can be used to determine the absorption edge energy, which is the band gap. We used a plot $[F(R) \cdot h\nu]^{1/2}$ vs. $h\nu$ to calculate the band gap values of TiO_2/CdS coatings [11]. The calculated band gap energy for all TiO_2/CdS coatings is at about 3.16 eV, except for TiO_2/CdS coating formed in electrolyte with addition of 8 g/L CdS powder which is at about 3.14 eV (Fig. 9).

The absence of adsorption shift might be attributed to a low concentration of CdS particles incorporated into coatings, which is also suggested by XRD, indicating that CdS particles are suppressing the recombination of photogenerated electron–hole pairs. On the other hand, if concentration of CdS particles incorporated into TiO_2 coatings is too high, it increases the concentration of recombination centers for electron–hole pairs, resulting in lower PA.

High sensitivity and nondestructive character render photoluminescence (PL) technique useful in the field of photocatalysis because information such as the efficiency of charge carrier trapping, migration and transfer can be obtained [22]. It is generally acknowledged that increase of PL intensity corresponds to decrease of photocatalytic activity, indicating fast recombination of electron-hole pairs. PL emission spectra of prepared coatings excited at 350 nm are shown in Fig. 10a. By raising the concentration of CdS particles in electrolyte up to 0.4 g/L, a decrease in PL intensity is observed, while further increase of CdS particles concentration in electrolyte up to 1.0 g/L results in increasing PL intensity. These results are in accordance with photocatalytic measurements (Fig. 10b), i.e., the decrease of PL intensity corresponds to increase of PA, indicating slower recombination of electron–hole pairs. For higher concentrations of CdS particles in supporting electrolyte (2 g/L and more), a simultaneous decrease of PL intensity and photocatalytic activity can be related to increasing presence of CdS dopants which become capture centers for photoinduced electrons.

Based on the above discussion, the following degradation mechanism of MO can be proposed [23-25]. Under the irradiation, electrons are excited from the valence band (VB) of CdS in TiO_2/CdS coatings to the conduction band (CB) of CdS, thus forming the electron–hole pairs. The position of CB and VB gap edges of CdS enables the injection of photoexcited electrons from CB of CdS into the low-lying CB of TiO_2. On the other hand, the holes generated in CdS valence band cannot be transferred to VB of TiO_2, because CdS valence band is more cathodic than that of TiO_2. The recombination between photogenerated electrons and holes is suppressed as a result of the separation effect, allowing more opportunities for electrons and holes to participate in oxidation-reduction reactions. Photogenerated electrons can react with the adsorbed O_2 to form radicals such as $^{\bullet}O_2^-$, $^{\bullet}OH$ and then these radicals further oxidize MO molecules to CO_2 and H_2O. Meanwhile, the holes can react with OH^- or H_2O to generate $^{\bullet}OH$ radicals, which can also take part in the degradation reactions of MO in the photocatalytic process.

It is also worth mentioning that over the past few years our group has applied PEO processing to couple TiO_2 with wide band gap semiconductors such as WO_3 [19], V_2O_5 [26], and SnO_2 [27] in order to improve the photocatalytic efficiency of TiO_2. Fig. 11 presents PA of above mentioned photocatalysts in MO degradation. Clearly, TiO_2/CdS photocatalyst is more efficient in degrading MO than TiO_2/V_2O_5 and TiO_2/SnO_2, while TiO_2/WO_3 still remains the most efficient mixed-oxide photocatalyst obtained by PEO processing.

4. Conclusions

In this work, for the first time we used plasma electrolytic oxidation (PEO) process for the formation of TiO_2/CdS photocatalysts on titanium substrate in alkaline electrolyte containing CdS particles. Unfortunately, the environmental friendliness of the PEO process in

electrolyte containing CdS particles is questionable because CdS is toxic, especially when inhaled, and cadmium compounds generally are classified as carcinogenic.

The surface morphology is not significantly influenced by the addition of CdS particles to the supporting electrolyte. The coatings are mainly composed of anatase TiO_2 phase. Raman spectroscopy confirmed inert incorporation of CdS particles into TiO_2 coatings. CdS particles inside TiO_2 coatings do not have influence on the absorption spectra which showed a band edge at about 385 nm.

Photocatalytic activity of TiO_2/CdS coatings is strongly dependent on the concentration of CdS particles in supporting electrolyte. The highest photocatalytic activity was observed for coatings formed in supporting electrolyte with addition of 0.4 g/L of CdS particles. Observed photocatalytic activity is considerably higher than that of pure TiO_2 coatings formed in supporting electrolyte under the same conditions. Enhanced photocatalytic activity is related to the reduced recombination rate of photogenerated electron/hole pairs as a result of coupling of TiO_2 and CdS.

Acknowledgements

This work is supported by the Ministry of Education, Science, and Technological Development of the Republic of Serbia under projects No. 171035 and 172022.

References

[1] A. Mills, S.L. Hunte, An overview of semiconductor photocatalysis, Journal of Photochemistry and Photobiology A: Chemistry 108 (1997) 1–35.

[2] M. Pelaez, N.T. Nolan, S.C. Pillai, M.K. Seery, P. Falaras, A.G. Kontos, P.S.M. Dunlop, J.W.J. Hamilton, J.A. Byrne, K. O'Shea, M.H. Entezari, D.D. Dionysiou, A review on the

visible light active titanium dioxide photocatalysts for environmental applications, Applied Catalysis B: Environmental 125 (2012) 331–349.

[3] A. Fujishima, T.N. Rao, D.A. Tryk, Titanium dioxide photocatalysis, Journal of Photochemistry and Photobiology C: Photochemistry Reviews 1 (2000) 1–21.

[4] S.G. Kumar, L.G. Devi, Review on modified TiO_2 photocatalysis under UV/Visible light: selected results and related mechanisms on interfacial charge carrier transfer dynamics, Journal of Physical Chemistry. Part A: Molecules, Spectroscopy, Kinetics, Environment and General Theory 115 (2012) 13211–13241.

[5] S.B. Rawal, S. Bera, D. Lee, D.J. Jang, W.I. Lee, Design of visible-light photocatalysts by coupling of narrow bandgap semiconductors and TiO_2: effect of their relative energy band positions on the photocatalytic effciency, Catalysis Science and Technology, 3 (2013) 1822–1830.

[6] X. Guo, C. Chen, W. Song, X. Wang, W. Di, W. Qin, CdS embedded TiO_2 hybrid nanospheres for visible light photocatalysis, Journal of Molecular Catalysis A: Chemical 387 (2014) 1–6.

[7] A. Meng, B. Zhu, B. Zhong, L. Zhang, B. Cheng, Direct Z-scheme TiO_2/CdS hierarchical photocatalyst for enhanced photocatalytic H_2-production activity, Applied Surface Science 422 (2017) 518–527.

[8] Z. Tian, N. Yu, Y. Cheng, Z. Wang, Z. Chen, L. Zhang, Hydrothermal synthesis of graphene/TiO_2/CdS nanocomposites as efficient visible-light-driven photocatalysts, Materials Letters 194 (2017) 172–175.

[9] S. Yu, J. Hu, J. Li, Self-assembly of TiO_2/CdS mesoporous microspheres with enhanced photocatalytic activity via hydrothermal method, International Journal of Photoenergy 2014 (2014) 854217.

[10] M. Khatamian, M.S. Oskoui, M. Haghighi, M. Darbandi, Visible-light response photocatalytic water splitting over CdS/TiO_2 and $CdS–TiO_2$/metalosilicate composites, International Journal of Energy Research, 38 (2014) 1712–1726.

[11] P. Prasannalakshmi, N. Shanmugam, Photocatalytic decolourization of brilliant green and methylene blue by TiO_2/CdS nanorods, Journal of Solid State Electrochemistry 21 (2017) 1751–1766.

[12] G. Yang, B. Yang, T. Xiao, Z. Yan, One-step solvothermal synthesis of hierarchically porous nanostructured CdS/TiO_2 heterojunction with higher visible light photocatalytic activity, Applied Surface Science 283 (2013) 402–410.

[13] S. Stojadinović, R. Vasilić, M. Perić, Investigation of plasma electrolytic oxidation on valve metals by means of molecular spectroscopy – a review, RSC Advances 4 (2014) 25759–25789.

[14] A.L. Yerokhin, X. Nie, A. Leyland, A. Matthews, S.J. Dowey, Plasma electrolysis for surface engineering, Surface and Coatings Technology 122 (1999) 73–93.

[15] X. Lu, M. Mohedano, C. Blawert, E. Matykina, R. Arrabal, K.U. Kainer, M.L. Zheludkevich, Plasma electrolytic oxidation coatings with particle additions – a review, Surface and Coatings Technology 307 (2016) 1165–1182.

[16] A. Sankhla, R. Sharma, R.S. Yadav, D. Kashyap, S.L. Kothari, S. Kachhwaha, Biosynthesis and characterization of cadmium sulfide nanoparticles - An emphasis of zeta potential behavior due to capping, Materials Chemistry and Physics 170 (2016) 44–51.

[17] S. Stojadinović, R. Vasilić, M. Petković, B. Kasalica, I. Belča, A. Žekić, Lj. Zeković, Characterization of the plasma electrolytic oxidation of titanium in sodium metasilicate, Applied Surface Science 265 (2013) 226–233.

[18] S. Stojadinović, N. Radić, B. Grbić, S. Maletić, P. Stefanov, A. Pačevski, R. Vasilić, Structural, photoluminescent and photocatalytic properties of TiO_2:Eu^{3+} coatings formed by plasma electrolytic oxidation, Applied Surface Science 370 (2016) 218–228.

[19] S. Stojadinović, N. Radić, R. Vasilić, M. Petković, P. Stefanov, L. Zeković, B.Grbić, Photocatalytic properties of TiO_2/WO_3 coatings formed by plasma electrolytic oxidation of titanium in 12-tungstosilicic acid, Applied Catalysis B Environmental 126 (2012) 334–341.

[20] C. Su, C. Shao, Y. Liu, Electrospun nanofibers of TiO_2/CdS heteroarchitectures with enhanced photocatalytic activity by visible light, Journal of Colloid and Interface Science 359 (2011) 220–227.

[21] A.G. Ilie, M. Scarisoareanu, I. Morjan, E. Dutu, M. Badiceanu, I. Mihailescu, Principal component analysis of Raman spectra for TiO_2 nanoparticle characterization, Applied Surface Science 417 (2017) 93–103.

[22] J. Liqiang, Q. Yichun, W. Baiqi, L. Shudan, J. Baojiang, Y. Libin, F. Wei, F. Honggang, S. Jiazhong, Review of photoluminescence performance of nano-sized semiconductor materials and its relationships with photocatalytic activity, Solar Energy Materials and Solar Cells 90 (2006) 1773–1787.

[23] X. Yang, Y. Wang, Z. Wang, X. Lv, H. Jia, J. Kong, M. Yu, Preparation of CdS/TiO_2 nanotube arrays and the enhanced photocatalytic property, Ceramics International 42 (2016) 7192–7202.

[24] L. Li, L. Wang, T. Hu, W. Zhang, X. Zhang, X. Chen, Preparation of highly photocatalytic active CdS/TiO_2 nanocomposites by combining chemical bath deposition and microwave-assisted hydrothermal synthesis, Journal of Solid State Chemistry 218 (2014) 81–89.

[25] C. Xue, T. Wang, G. Yang, B. Yang, S. Ding, A facile strategy for the synthesis of hierarchical TiO_2/CdS hollow sphere heterostructures with excellent visible light activity, Journal of Materials Chemistry A 2 (2014) 7674–7679.

[26] R. Vasilić, S. Stojadinović, N. Radić, P. Stefanov, Z. Dohčević-Mitrović, B. Grbić, One-step preparation and photocatalytic performance of vanadium doped TiO_2 coatings, Materials Chemistry and Physics 151 (2015) 337–344.

[27] S. Stojadinović, N. Tadić, N. Radić, B. Grbić, R. Vasilić, TiO_2/SnO_2 photocatalyst formed by plasma electrolytic oxidation, Materials Letters 196 (2017) 292–295.

Figure Captions:

Figure 1. Size distribution of CdS particles.

Figure 2. SEM micrographs of coatings formed by PEO in supporting electrolyte with addition of various concentration of CdS particles (a) 0.0 g/L; (b) 0.1 g/L; (c) 0.2 g/L; (d) 0.3 g/L; (e) 0.4 g/L, (f) 0.5 g/L; (g) 1.0 g/L, (h) 2.0 g/L; (i) 4.0 g/L, (j) 8.0 g/L.

Figure 3. SEM micrograph of polished cross-section of coating formed in supporting electrolyte with addition of 8.0 g/L of CdS particles.

Figure 4. (a) XRD pattern of used CdS particles; (b) XRD patterns of coatings formed in supporting electrolyte with addition of various concentrations of CdS particles.

Figure 5. Raman spectra of CdS particles, TiO_2 coating formed in supporting electrolyte, and TiO_2/CdS coating formed in supporting electrolyte with addition of 8 g/L CdS particles.

Figure 6. High resolution SEM micrograph of coating formed in supporting electrolyte with addition of 8 g/L CdS particles.

Figure 7. Photocatalytic performance of TiO_2/CdS coatings formed in supporting electrolyte with addition of various concentrations of CdS particles.

Figure 8. DRS spectra of CdS particles and the coatings formed in supporting electrolyte with addition of various concentrations of CdS particles.

Figure 9. Tauc plots of TiO_2/CdS coatings formed in supporting electrolyte with addition of various concentrations of CdS particles.

Figure 10. (a) PL emission spectra excited at 350 nm of TiO_2/CdS coatings formed in supporting electrolyte with addition of various concentration of CdS particles; (b) Influence of CdS concentration in supporting electrolyte on: PL intensity at 425 nm and PA after 12 hours of irradiation of TiO_2/CdS coatings.

Figure 11. Photocatalytic degradation of MO using various photocatalysts.

Table Captions:

Table 1. Ti/Cd ratio detected in TiO_2/CdS coatings formed in supporting electrolyte with addition of various concentrations of CdS particles.

CdS (g/L)	0.0	0.1	0.2	0.3	0.4	0.5	1.0	2.0	4.0	8.0
Cd/Ti (10^{-4})	0	4.01	4.23	4.35	4.52	4.83	5.23	6.35	7.47	9.48

Highlights

- PEO coatings are formed on titanium in CdS powder containing electrolytes.
- PEO coatings are mostly composed of anatase phase of TiO_2.
- Concentration of CdS particles is an important factor affecting photocatalytic activity.
- Coating formed with 0.4 g/L CdS electrolyte showed the best photocatalytic activity.

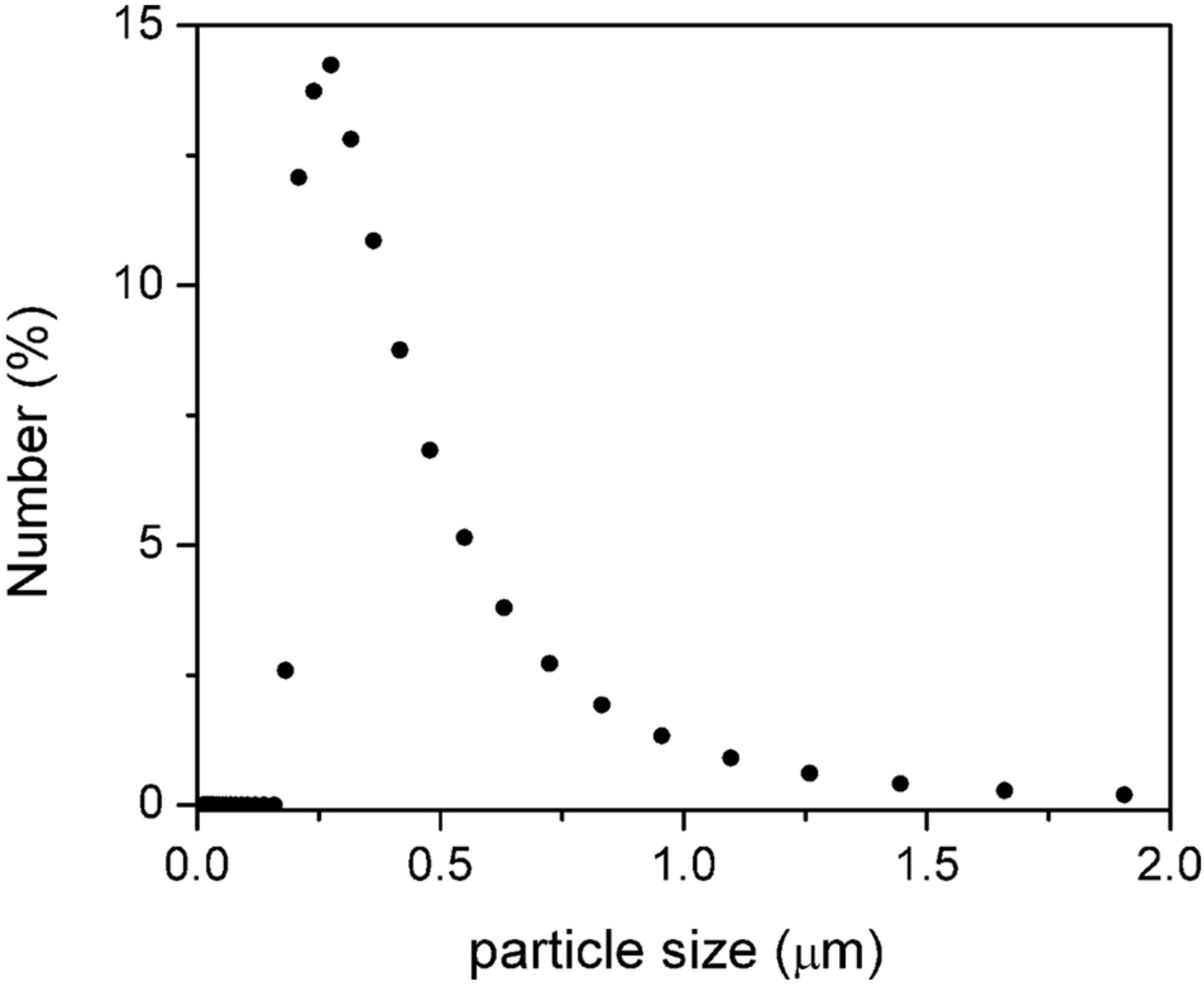

Figure 1

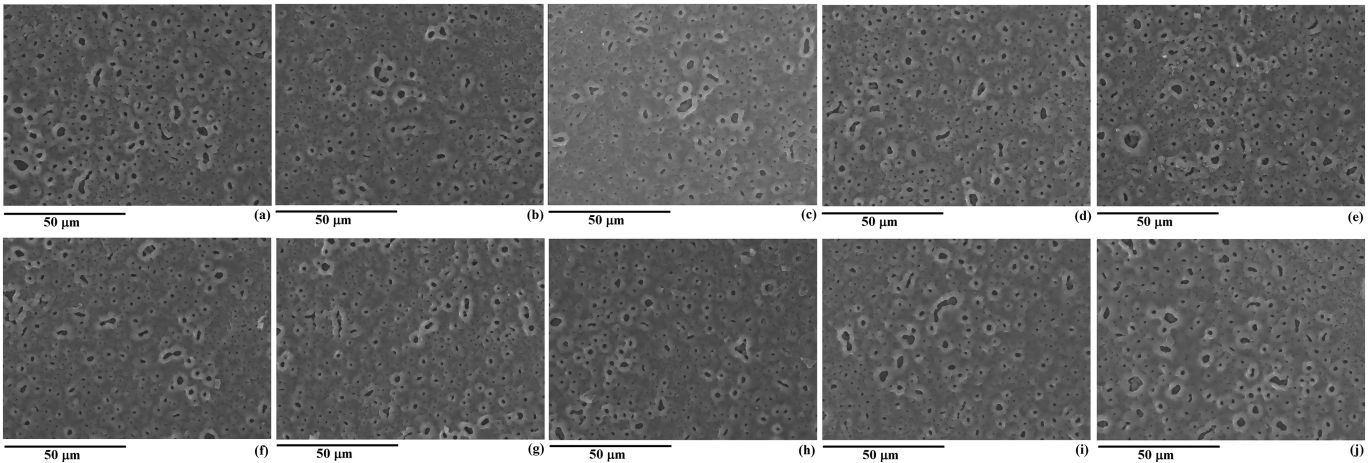
50 μm
(a)
50 μm
(b)
50 μm
(c)
50 μm
(d)
50 μm
(e)
50 μm
(f)
50 μm
(g)
50 μm
(h)
50 μm
(i)
50 μm
(j)

Figure 2

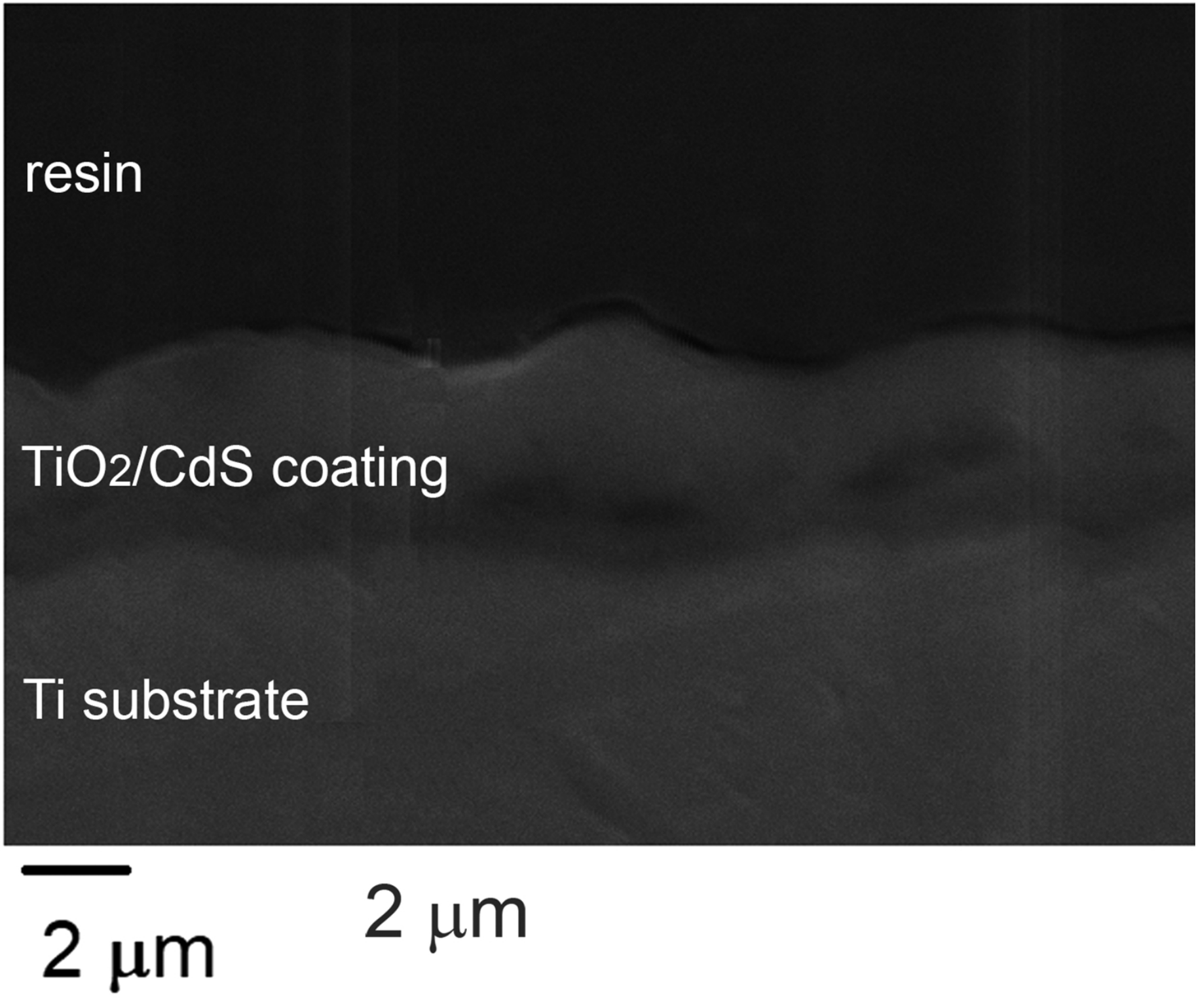

Figure 3

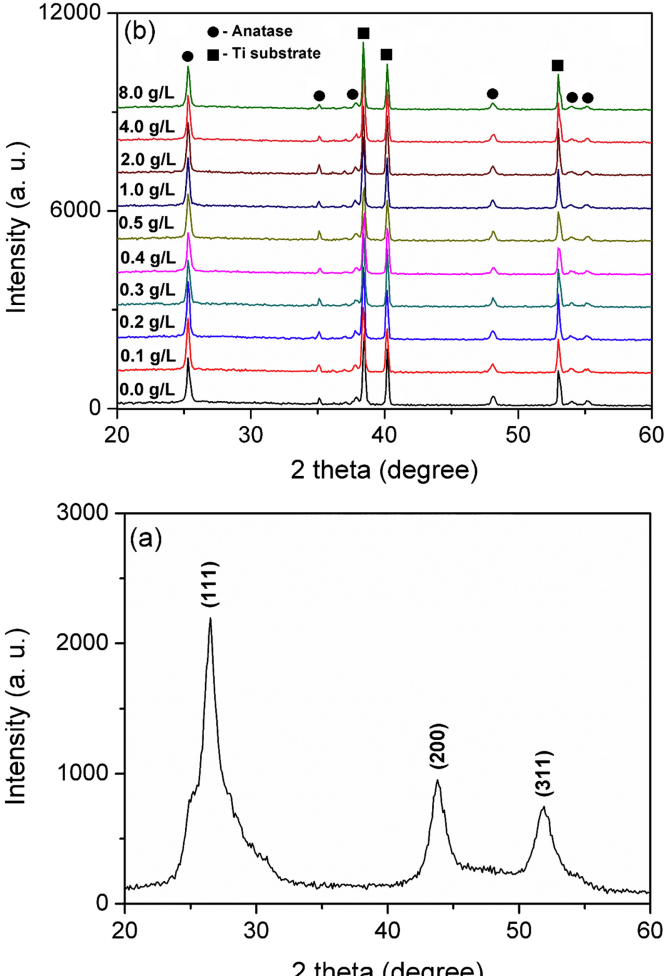
(b)
● - Anatase
■ - Ti substrate
8.0 g/L
4.0 g/L
2.0 g/L
1.0 g/L
0.5 g/L
0.4 g/L
0.3 g/L
0.2 g/L
0.1 g/L
0.0 g/L
Intensity (a. u.)
2 theta (degree)
(a)
(111)
(200)
(311)
Intensity (a. u.)
2 theta (degree)

Figure 4

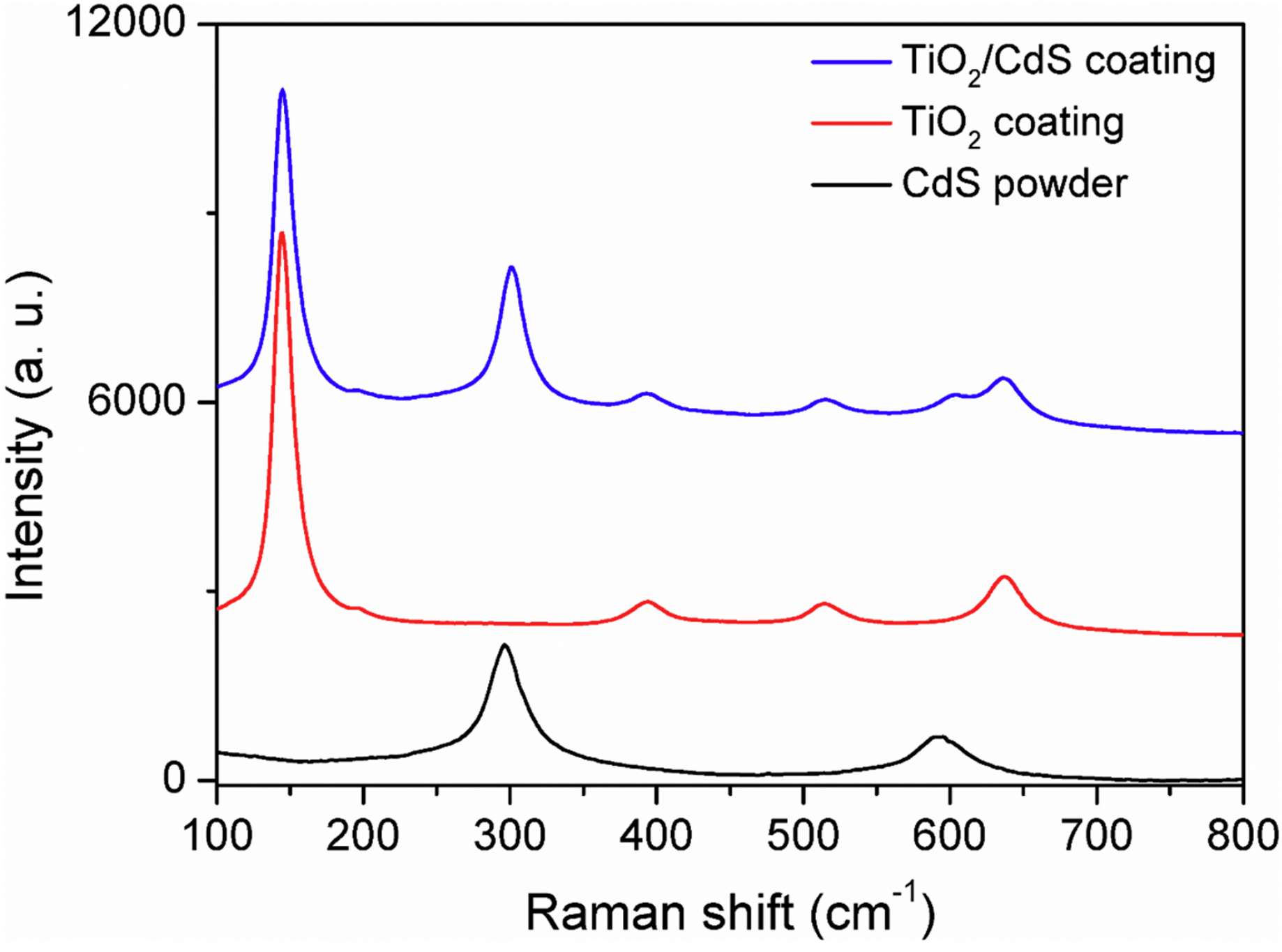
12000
6000
0
Intensity (a. u.)
100
200
300
400
500
600
700
800
Raman shift (cm-1)
TiO2/CdS coating
TiO2 coating
CdS powder

Figure 5

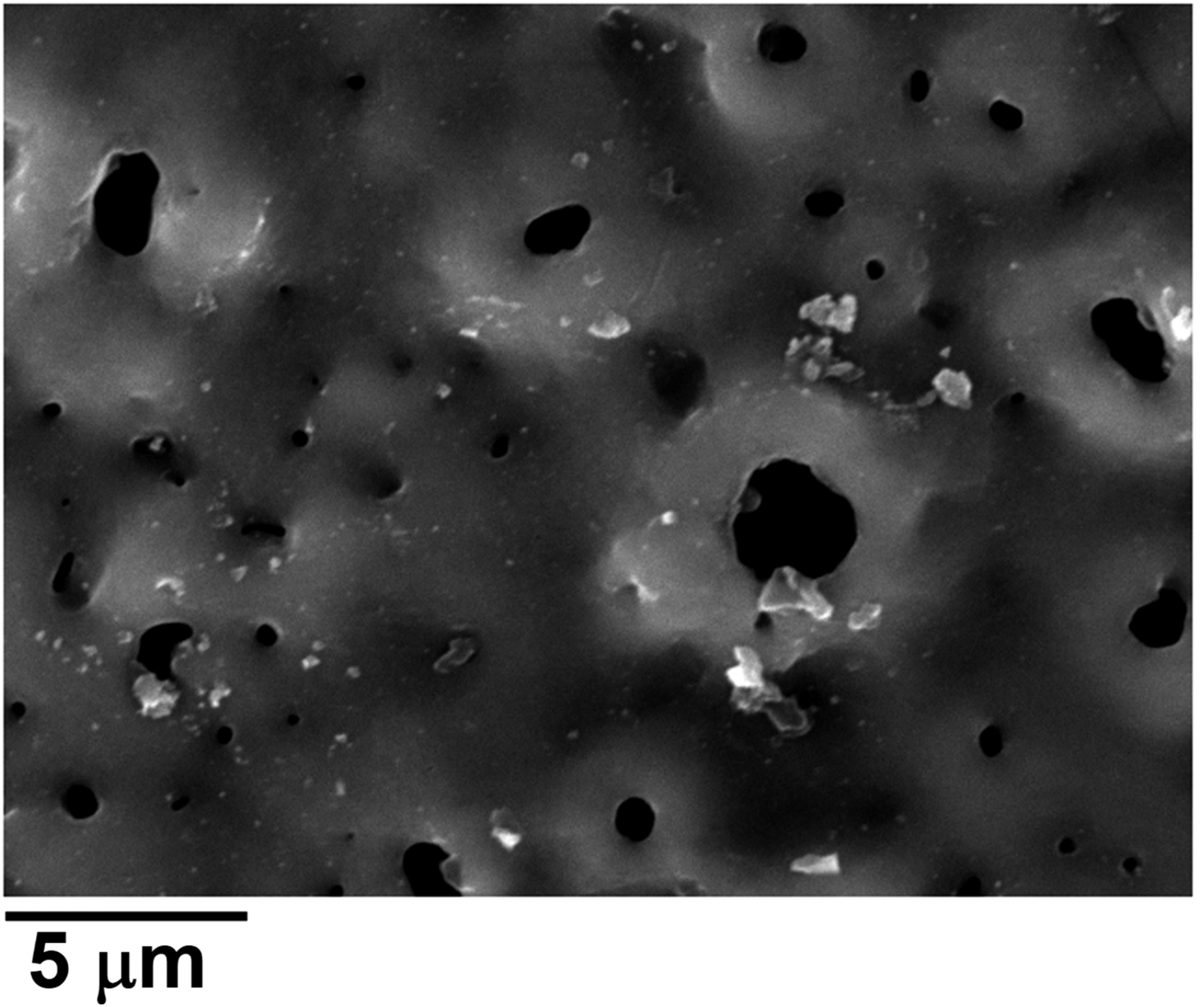

Figure 6

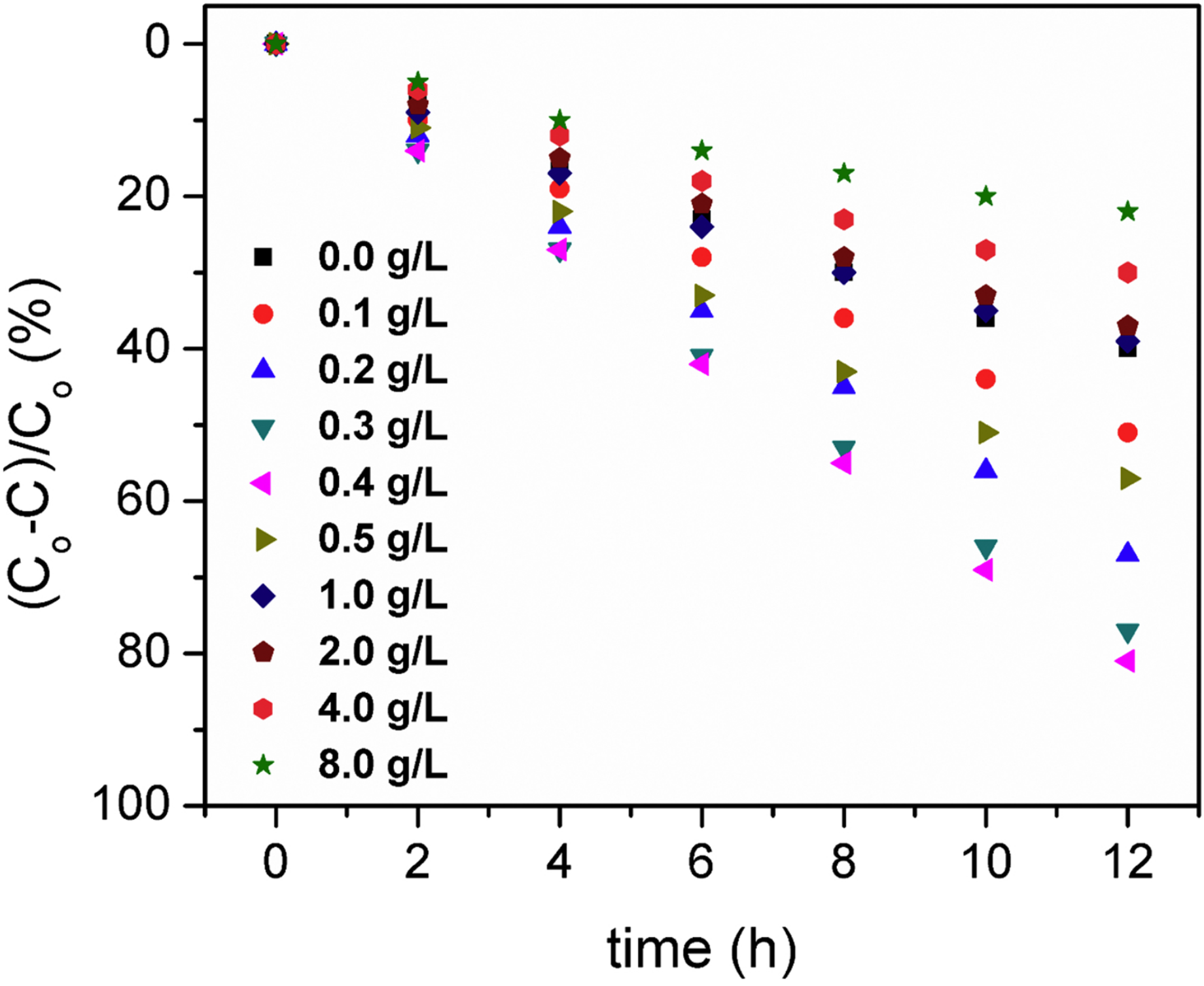
0
20
40
60
80
100
(C$_o$-C)/C$_o$ (%)
0.0 g/L
0.1 g/L
0.2 g/L
0.3 g/L
0.4 g/L
0.5 g/L
1.0 g/L
2.0 g/L
4.0 g/L
8.0 g/L
0
2
4
6
8
10
12
time (h)

Figure 7

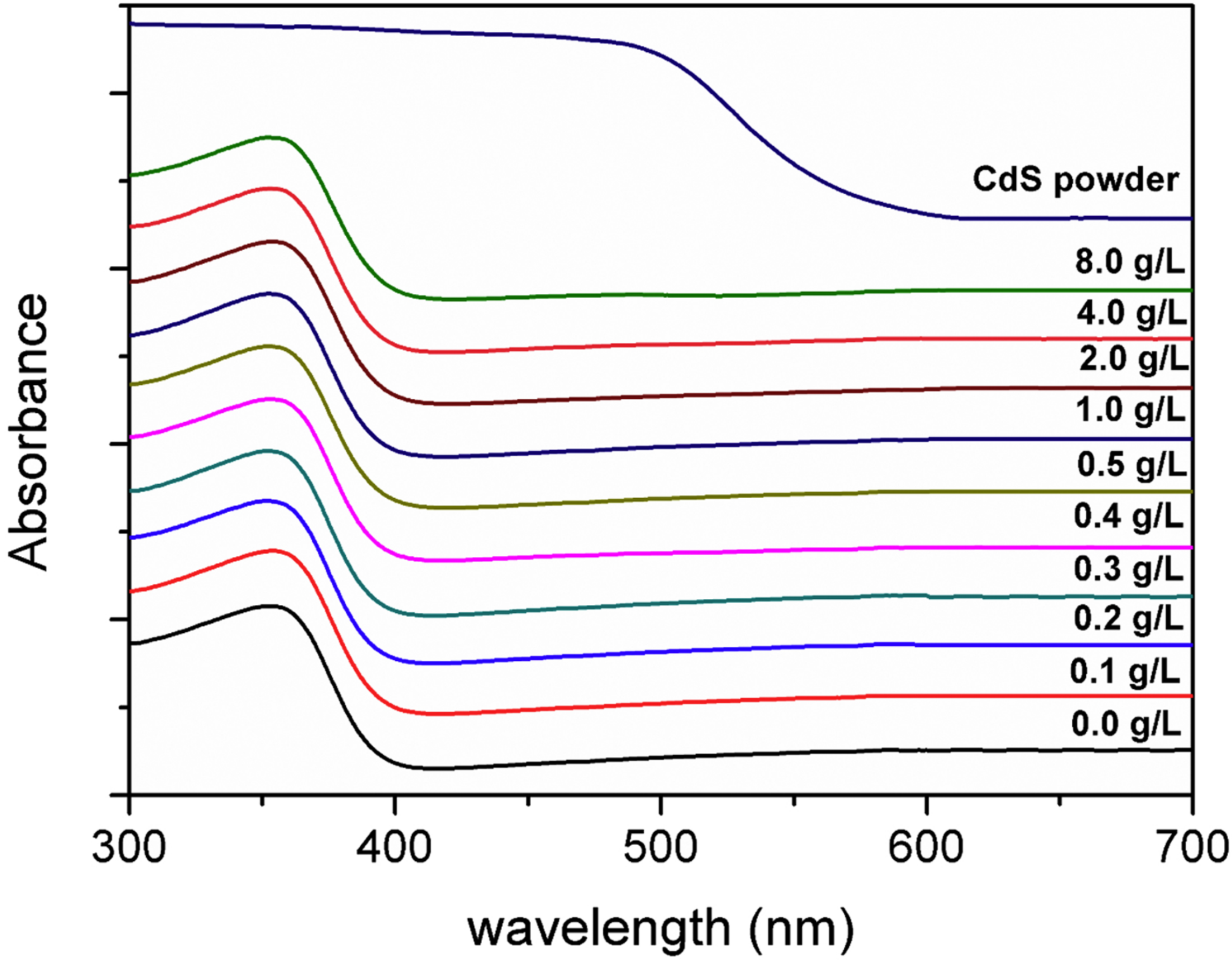
CdS powder
8.0 g/L
4.0 g/L
2.0 g/L
1.0 g/L
0.5 g/L
0.4 g/L
0.3 g/L
0.2 g/L
0.1 g/L
0.0 g/L
Absorbance
300
400
500
600
700
wavelength (nm)

Figure 8

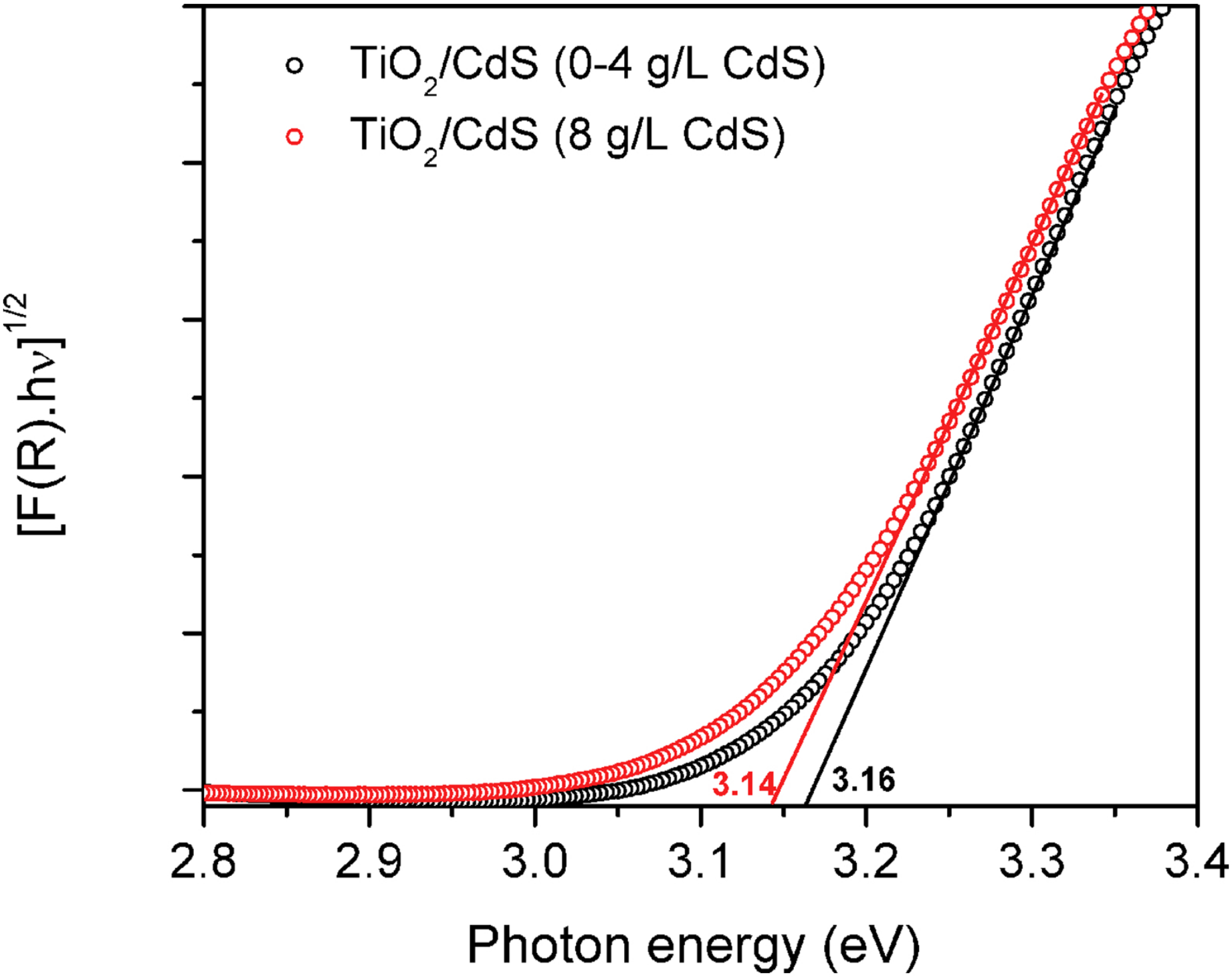
TiO2/CdS (0-4 g/L CdS)
TiO2/CdS (8 g/L CdS)
[F(R).hν]1/2
3.14
3.16
2.8
2.9
3.0
3.1
3.2
3.3
3.4
Photon energy (eV)

Figure 9

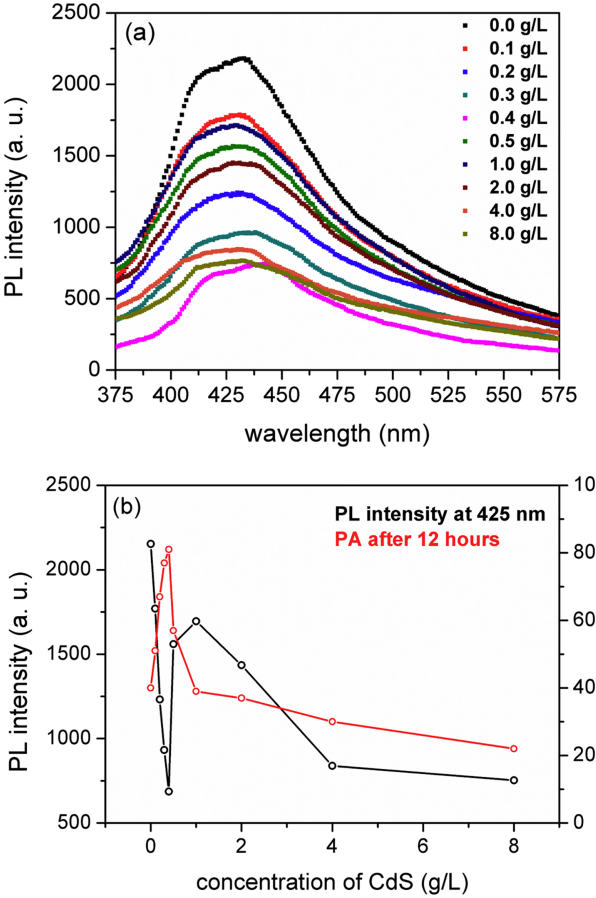
(a)
0.0 g/L
0.1 g/L
0.2 g/L
0.3 g/L
0.4 g/L
0.5 g/L
1.0 g/L
2.0 g/L
4.0 g/L
8.0 g/L
PL intensity (a. u.)
wavelength (nm)
(b)
PL intensity at 425 nm
PA after 12 hours
PL intensity (a. u.)
(C-C$_0$)/C$_0$ (%)
concentration of CdS (g/L)

Figure 10

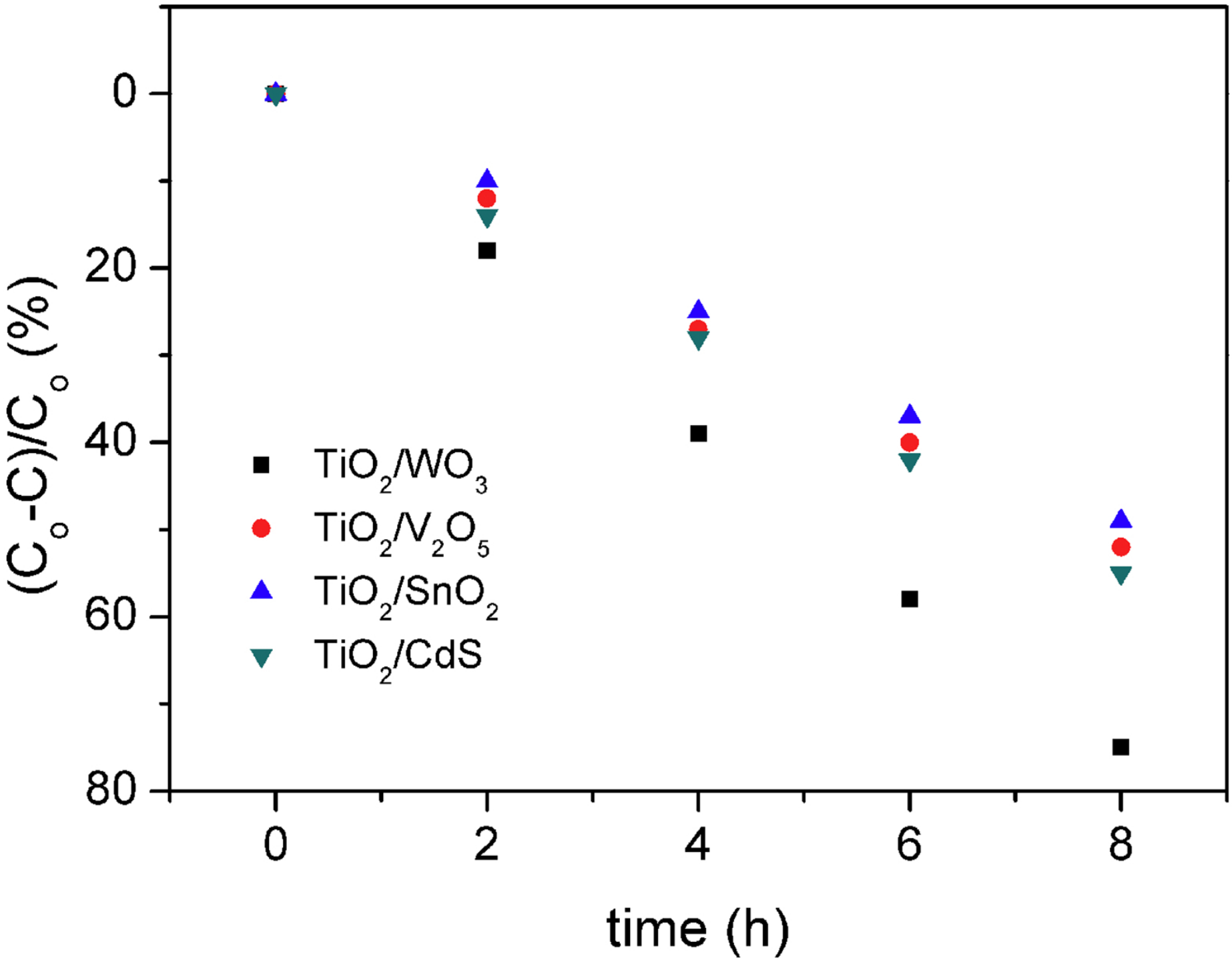
0
20
40
60
80
(C$_o$-C)/C$_o$ (%)
0
2
4
6
8
time (h)
TiO$_2$/WO$_3$
TiO$_2$/V$_2$O$_5$
TiO$_2$/SnO$_2$
TiO$_2$/CdS

Figure 11